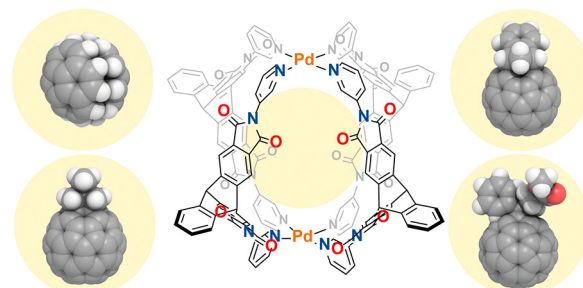


Guest Encapsulation Scope of a Triptycene-Based Pd₂L₄ Coordination Cage

Shota Hasegawa^a Ananya Baksi^a Bin Chen^{a,b} Guido H. Clever^{*a} ^a Department of Chemistry and Chemical Biology, TU Dortmund University, Otto-Hahn Str. 6, 44227 Dortmund, Germany^b State Key Laboratory of Radiation Medicine and Protection, Collaborative Innovation Center of Radiation Medicine of Jiangsu Higher Education Institutions, Soochow University, Suzhou, P. R. of China

* guido.clever@tu-dortmund.de



Aromatic and fullerene-based guests are encapsulated inside a triptycene-based coordination cage

Received: 16.08.2022

Accepted after revision: 16.09.2022

DOI: 10.1055/a-1953-0155; Art ID: OM-2022-08-0033-SC

License terms:

© 2022. The Author(s). This is an open access article published by Thieme under the terms of the Creative Commons Attribution-NonDerivative-NonCommercial License, permitting copying and reproduction so long as the original work is given appropriate credit. Contents may not be used for commercial purposes, or adapted, remixed, transformed or built upon. (<https://creativecommons.org/licenses/by-nc-nd/4.0/>)

Abstract The scope of a lantern-shaped, triptycene-based Pd₂L₄ coordination cage to encapsulate various carbon-rich guests was investigated. The cage was found to bind two molecules of corannulene and a variety of C₆₀ derivatives in moderate to quantitative yields. Non-disruptive extraction of encapsulated fullerene derivative PC₆₁BM from the cage was demonstrated by the simple addition of CS₂ into an acetonitrile solution of the host–guest complex. This process can be accomplished in a layer-to-layer fashion, and thus, the recovered cage can be further utilized in a recycling process. As this self-assembled host is readily synthesized and able to transfer fullerenes and a range of its derivatives into polar organic solvents, it allows facilitating purification, chemical modification and solid-state processing of fullerenes for a range of materials applications.

Key words: supramolecular chemistry, host–guest complexes, fullerenes

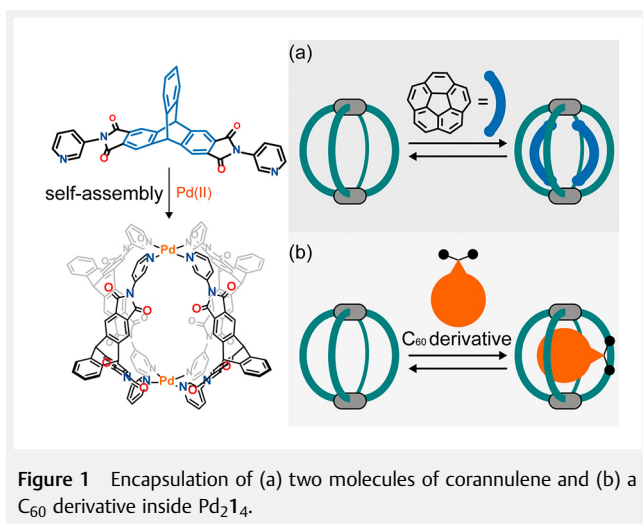
Introduction

Fullerene C₆₀ is a spherical molecular allotrope of carbon with plenty of applications.¹ For instance, the carbonaceous ball is a widely used electron-accepting material in photovoltaics.² Tuning of the molecular orbital energies of C₆₀ (and its derivatives) is a critical factor to tune the efficiency of exciton and electron transfer processes in materials for molecular electronics and photovoltaics.³ Chemical modification of C₆₀ can be employed to tune both its electronic structure as well as its solubility and mode of embedding into composite materials, thus, many reactions to chemically modify C₆₀ have been developed.^{4,5} For instance, PC₆₁BM

(**4**) is one of the most utilized C₆₀ derivatives as an electron-accepting material.⁶ While covalent modification is a straightforward way to tune the electronic properties of C₆₀, chemical reactions that produce stereochemically defined products are often difficult to control due to a comparable reactivity of carbon positions on pure C₆₀ and its derivatives, causing the formation of multi-adduct isomers.^{6,7} To achieve regio-controlled modification, various strategies have been developed such as tether-directed syntheses and supramolecular masking methods.^{8–16} Furthermore, examples of C₆₀ derivative encapsulation inside coordination cages have been reported.^{17–19} Among them, especially the coordination cages reported by Ribas and Yoshizawa were examined for their propensity to encapsulate and release C₆₀ derivatives.^{17,19}

Tailored purification methods for C₆₀ derivatives are still scarce, and thus, there is demand for further strategies to be explored. Recently, our group has reported a new family of coordination cages based on organic ligands having a curved π-surface.^{20–23} These self-assembled hosts provide a cavity of suitable size and shape to strongly bind C₆₀/C₇₀ via convex-concave π-interactions. Tight encapsulation of fullerenes inside these cages allows for a multitude of applications. For example, the generation and long-term stabilization of the C₆₀^{•−} radical anion by nano-confinement inside triptycene-based cage Pd₂L₄ in organic solvents has been demonstrated.²³

For some reported coordination cages composed of ligands with curved π-surfaces, binding of carbon-rich guests has been demonstrated in the past²⁴; however, the encapsulation capability of Pd₂L₄ has only been investigated for C₆₀ so far. We envisaged that this coordination cage should be able to accommodate not only pristine C₆₀, but also other carbon-rich guest compounds including C₆₀ derivatives. Stimulated by the idea of widening the scope of guest uptake, the encapsulation capability of Pd₂L₄ has been further investigated in the herein-described study (Figure 1). In the course of this study, Pd₂L₄ was found to be capable of encapsulating



solating two molecules of corannulene (Figure 1a). Furthermore, Pd_214 displayed high to quantitative affinity towards a variety of C_{60} derivatives such as $PC_{61}BM$ (Figure 1b). Stimulated by the fact that Pd_214 can encapsulate $PC_{61}BM$ but not $PC_{62}BM$, which is a bis-adduct analogue of $PC_{61}BM$, we explored a facile method to purify $PC_{61}BM$ by selective uptake and extraction from the cavity. We herein report that addition of CS_2 is able to liberate encapsulated $PC_{61}BM$ from the cage in a recycling, yet non-disruptive, manner.

Results and Discussion

The triptycene-based Pd_2L_4 coordination cage was prepared following our previous work.²³ We started investigating the guest scope of Pd_214 with a selection of rather small neutral polyaromatic hydrocarbons (for details, see Figures S24 and S25). Among these, only corannulene, representing a sub-structure of C_{60} , was found to be encapsulated within the cavity (Figure 2a). In detail, an excess amount of powdered corannulene was added into an acetonitrile solution of Pd_214 and heated at 70 °C for 24 h.²⁵ In the 1H NMR spectrum, a new set of peaks which could be assigned to $(Cor)_2@Pd_214$ was observed besides parental Pd_214 , which means that encapsulation of corannulene occurs pairwise in a cooperative fashion with exchange kinetics slower than the NMR time scale (Figure 2b). Two molecules of corannulene were found to be incorporated inside Pd_214 according to the 1H NMR signal integration ratio between host and guest signals and the results of a NOESY experiment (Figures S28 and S30). Noteworthy, the signals assigned to the Pd_214 host not containing the corannulene pair showed slightly different chemical shifts as compared to the cage sample in the absence of corannulene. We assume that this is caused by loose encapsulation of a single corannulene in fast exchange for this fraction of species in the equilibrium.

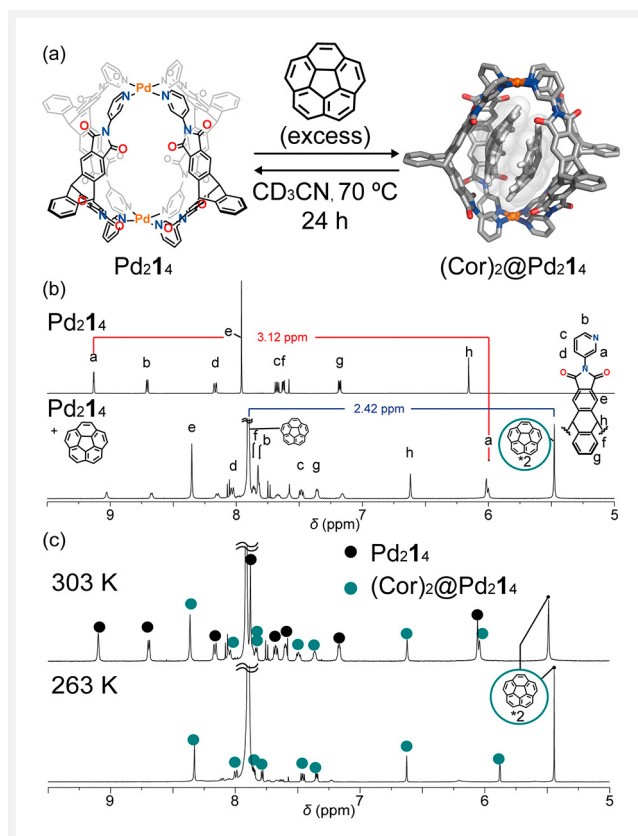


Figure 2 (a) Encapsulation of corannulenes inside Pd_214 . An optimized geometry is shown for $(Cor)_2@Pd_214$. (b) 1H NMR spectra (CD_3CN , 0.7 mM, 500 MHz, 298 K) of Pd_214 (top) and Pd_214 with excess amount of corannulene (bottom). (c) 1H NMR spectra (CD_3CN , 500 MHz) of $(Cor)_2@Pd_214$ at 303 K (top) and at 263 K (bottom).

The protons of the encapsulated corannulene guests display an upfield shift by 2.42 ppm compared to the free corannulene existing in the solution, comparable to what was observed with other hosts.^{24,26} In addition, the H^a signal of the pyridine donors, pointing inward the cavity, also undergoes an upfield shift by 3.12 ppm, probably due to direct interactions between corannulene and these hydrogen substituents, further supporting the encapsulation of corannulene within the cavity.²³ Furthermore, diffusion-ordered spectroscopy (DOSY) analysis revealed that the encapsulated corannulenes show a smaller diffusion coefficient compared to free corannulene in the same acetonitrile solution (Figure S31). Further, encapsulation was found to be strongly temperature-dependent. Upon cooling, the ratio of $(Cor)_2@Pd_214$ increased from 39% (303 K) up to 77% (253 K, both at 0.70 mM cage concentration and excess of powdered corannulene). Intriguingly, during the VT- 1H NMR experiment, a host-guest complex of Pd_214 and single corannulene, namely $Cor@Pd_214$, was not observed as a distinguishable species (Figure 2c). To elucidate the dynamic behavior

of guest exchange, a ^1H NMR titration experiment was performed (Figure S37). Aliquots of an acetonitrile solution of corannulene were titrated into an acetonitrile solution of $\text{Pd}_2\mathbf{1}_4$. As a result, peaks assigned to the host–guest complex (Cor) $_2$ @ $\text{Pd}_2\mathbf{1}_4$ appeared over the addition of 7 equiv of corannulene, alongside with all remaining peaks of $\text{Pd}_2\mathbf{1}_4$ showing slight shifts ($\Delta\delta_{\text{max}} = -0.02$ ppm), probably indicating a fast equilibrium of the empty host with a labile mono-guest adduct.

To gain a further insight into this process, density functional theory (DFT) calculations at the M06-2X/Lan12dz level of theory were performed. As a result, encapsulation of two corannulene molecules was found to lead to a more than two times higher gain in stabilization energy than encapsulation of only a single corannulene inside the host (Table S2). In the calculated geometry, convex–concave interactions between the encapsulated corannulenes and the ligands are clearly visible.

Next, we investigated the encapsulation of various C_{60} derivatives inside $\text{Pd}_2\mathbf{1}_4$. Therefore, C_{60} derivatives were dispersed in an acetonitrile solution of $\text{Pd}_2\mathbf{1}_4$ at 70°C for 48 h, after which the residual powdered C_{60} derivative remains were removed. Compounds **2–4**, comprising different C_{60} mono-adducts, were bound in 87–100% yield, determined by ^1H NMR analyses measured at 298 K (Figure 3a,b).²⁷ In the ^1H NMR spectra of the resulting solutions, a new set of signals was found besides empty $\text{Pd}_2\mathbf{1}_4$. As shown in Figure 3a, the cage should be desymmetrized due to the encapsulation of these C_{60} derivatives, containing a rather bulky substituent. Indeed, in the ^1H NMR spectra of **2–4**@ $\text{Pd}_2\mathbf{1}_4$, two sets and four sets of signals were observed for the pyridine and triptycene-backbone protons, respectively, which indicates the encapsulation of the C_{60} derivatives with slow exchange dynamics (see Figure 3c and Figures S2, S8 and S16 for complete NMR assignments). In addition, DOSY ^1H NMR shows that all of the newly appearing signals belong to a single species, having a similar hydrodynamic radius to C_{60} @ $\text{Pd}_2\mathbf{1}_4$ (Figures S5, S13, and S21).²³ The formation of the host–guest complexes was further confirmed by ESI-MS measurements (Figure 3d). The encapsulation yield of **4** was 87% under the chosen conditions, while quantitative encapsulation of **2** was achieved. In addition, the small apertures found in the densely packed, modelled geometry of **4**@ $\text{Pd}_2\mathbf{1}_4$ suggested that encapsulation of bulkier derivatives such as PC_{62}BM , which can be found as side-products in the course of the synthesis of **4**, should not be possible (Figure 4a,b).⁶ To test this hypothesis, an excess amount of PC_{62}BM , available as a mixture of regio-isomers, was dispersed in an acetonitrile solution of $\text{Pd}_2\mathbf{1}_4$ for 24 h at 70°C . In the resulting ^1H NMR spectrum, only one set of signals for empty $\text{Pd}_2\mathbf{1}_4$ was observed (Figure S45). Hence, for steric reasons the bis-adduct does not seem to be able to bind. This result implies that $\text{Pd}_2\mathbf{1}_4$ is able to recognize C_{60} mono-adducts over corresponding bis-adducts. In fact,

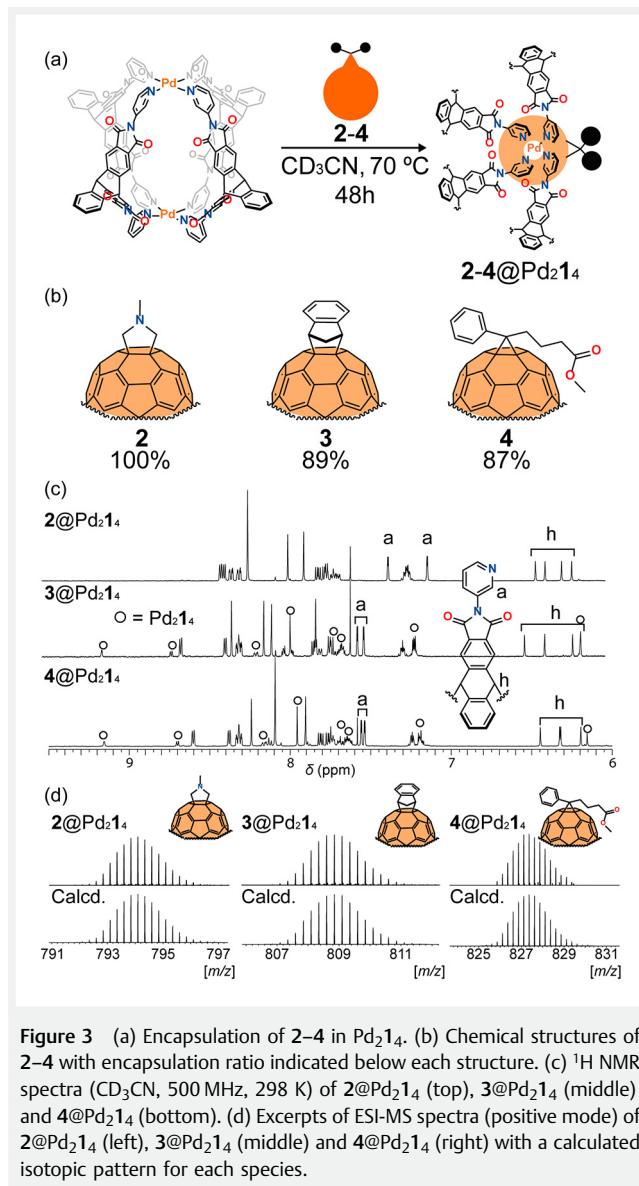


Figure 3 (a) Encapsulation of **2–4** in $\text{Pd}_2\mathbf{1}_4$. (b) Chemical structures of **2–4** with encapsulation ratio indicated below each structure. (c) ^1H NMR spectra (CD_3CN , 500 MHz, 298 K) of **2**@ $\text{Pd}_2\mathbf{1}_4$ (top), **3**@ $\text{Pd}_2\mathbf{1}_4$ (middle) and **4**@ $\text{Pd}_2\mathbf{1}_4$ (bottom). (d) Excerpts of ESI-MS spectra (positive mode) of **2**@ $\text{Pd}_2\mathbf{1}_4$ (left), **3**@ $\text{Pd}_2\mathbf{1}_4$ (middle) and **4**@ $\text{Pd}_2\mathbf{1}_4$ (right) with a calculated isotopic pattern for each species.

when the same equimolar amount of **4** and PC_{62}BM were dispersed in an acetonitrile solution of $\text{Pd}_2\mathbf{1}_4$ (with minute amounts of CS_2 as an additive to accelerate guest uptake in the heterogeneous system) at room temperature for 24 h, **4**@ $\text{Pd}_2\mathbf{1}_4$ was obtained as a major species (66% encapsulation yield), but again no host–guest complex with PC_{62}BM was formed. As can be seen in the molecular model of **4**@ $\text{Pd}_2\mathbf{1}_4$ calculated by DFT, the four ligands are forced close together to leave an enough space for accommodating the single appendix of **4** (Figure 4a,b). We assume that this structural detail then precludes encapsulation of bulkier PC_{62}BM . Often, encapsulation of lipophilic guest molecules such as fullerenes within a coordination cage dissolved in a very polar solvent is governed by solvophobic interactions,

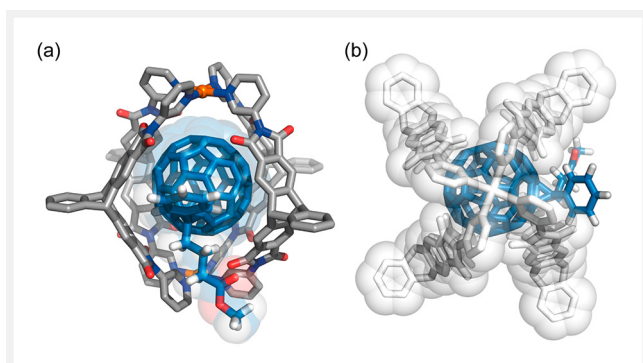


Figure 4 Optimized geometry of $4@Pd_214$ obtained by gas-phase DFT calculations at the B3LYP/LanL2dz level of theory for Pd atoms and 6–31 G(d,p) for all other atoms; (a) front and (b) top views.

as these guests prefer a rather non-polar cavity environment.²⁸ Therefore, addition of a better solvent for C_{60} to the host–guest complex solution was envisaged to shift the equilibrium between confined guest and free guest towards releasing of the guest molecule into the solvent.

Based on this assumption, we tested a variety of solvents which are commonly utilized to solubilize C_{60} . Indeed, addition of CS_2 was found to liberate encapsulated guest **4**. Once 33 vol% of CS_2 was added to an acetonitrile solution of $4@Pd_214$, the mixture was shaken and was left to stand for a few minutes. After this period of resting time, two layers were obtained, where the upper layer is a transparent acetonitrile solution of the empty coordination cage and the bottom layer is a reddish CS_2 solution containing the liberated compound **4** (Figure 5). The purity of the extracted guest molecule was confirmed by 1H NMR measurement (Figure S44). Note that this method is non-disruptive with respect to the host system, as can be seen in the 1H NMR spectrum of intact Pd_214 recovered from the upper layer (Figure S43). Finally, we challenged the repetitive encapsulation and release of **4** over 4 cycles (Table S3). After extract-

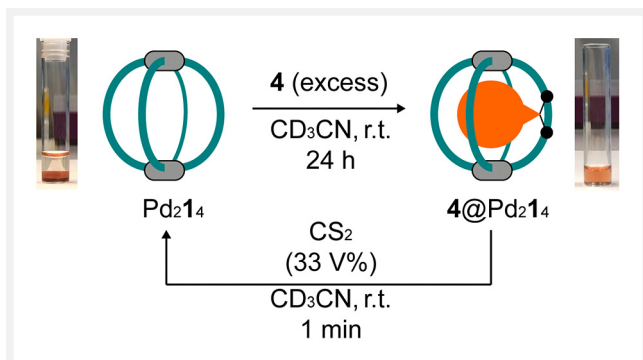


Figure 5 Recycling encapsulation and release of **4** using Pd_214 ; $4@Pd_214$ was obtained in 80.5%, 80.3%, 62.9%, and 52.2% yields after the 1st to 4th cycle, respectively. The yields were determined by 1H NMR.

ing **4** from $4@Pd_214$, the mixture was cooled to $-78^\circ C$ (to conveniently freeze the acetonitrile) and the CS_2 layer was removed by decanting. The recovered acetonitrile solution containing Pd_214 was further utilized for the next extraction experiment. Although a decline of the encapsulation yield was observed over repetitive cycles, Pd_214 was proven to accommodate and liberate **4** in a recycling yet non-disruptive manner (Figure 5). We presume that the observed decrease of the encapsulation yield can be attributed to losing some host by a slight miscibility of CS_2 in the acetonitrile solution.

Conclusions

We have investigated the encapsulation capability of coordination cage Pd_214 towards corannulene and several C_{60} -derivatives. Owing to the curved π -surface of the triptycene backbone of **1**, Pd_214 can encapsulate such non-planar aromatic compounds in high to quantitative yields. Pd_214 binds two molecules of corannulene in solution. Furthermore, Pd_214 incarcerates C_{60} derivatives **2–4**, all mono-adducts of C_{60} , in a way that the guests' substituents point outside the cavity through the space between the ligands, leading to a breaking of the fourfold symmetry of the cage. Encapsulation and liberation of **4** utilizing Pd_214 were demonstrated in a recycling manner. The recycling process can be accomplished in a layer-to-layer fashion, using two different solvents. In addition, Pd_214 does not encapsulate bulkier bis-adducts of fullerene derivatives, which should make Pd_214 a candidate for potent and sustainable fullerene derivative purification systems.

Funding Information

This work was funded by the Deutsche Forschungsgemeinschaft (DFG, German Research Foundation), under Germany's Excellence Strategy EXC 2033 – Project No. 390677874 – RESOLV and GRK2376 “Confinement-controlled Chemistry” – Project No. 331 085 229.

Acknowledgements

S.H. thanks the DAAD for a Ph.D. fellowship. We thank Prof. W.G. Hiller for assistance with NMR measurements.

Supporting Information

Supporting Information for this article is available online at <https://doi.org/10.1055/a-1953-0155>.

Conflict of Interest

The authors declare no conflict of interest.

References and Notes

- Kroto, H. W.; Heath, J. R.; O'Brien, S. C.; Curl, R. F.; Smalley, R. E. *Nature* **1985**, *318*, 162.
- Brabec, C. J.; Gowrisanker, S.; Halls, J. J. M.; Laird, D.; Jia, S.; Williams, S. P. *Adv. Mater.* **2010**, *22*, 3839.
- Umeyama, T.; Imahori, H. *Acc. Chem. Res.* **2019**, *52*, 2046.
- Nierengarten, J.-F. *New J. Chem.* **2004**, *28*, 1177.
- Itami, K. *Chem. Rec.* **2011**, *11*, 226.
- Hummelen, J. C.; Knight, B. W.; LePeq, F.; Wudl, F.; Yao, J.; Wilkins, C. L. *J. Org. Chem.* **1995**, *60*, 532.
- Puplovskis, A.; Kacens, J.; Neilands, O. *Tetrahedron Lett.* **1997**, *38*, 285.
- Isaacs, L.; Haldimann, R. F.; Diederich, F. *Angew. Chem. Int. Ed. Engl.* **1994**, *33*, 2339.
- Thilgen, C.; Diederich, F. *Chem. Rev.* **2006**, *106*, 5049.
- Maxouti, K. L.; Hirsch, A. *Eur. J. Org. Chem.* **2018**, *2018*, 2579.
- Fuertes-Espinosa, C.; García-Simón, C.; Pujals, M.; Garcia-Borràs, M.; Gómez, L.; Parella, T.; Juanhuix, J.; Imaz, I.; MasPOCH, D.; Costas, M.; Ribas, X. *Chem* **2019**, *6*, 169.
- Leonhardt, V.; Fimmel, S.; Krause, A.-M.; Beuerle, F. *Chem. Sci.* **2020**, *11*, 8409.
- Hasegawa, S.; Clever, G. H. *Chem* **2020**, *6*, 5.
- Ubasart, E.; Borodin, O.; Fuertes-Espinosa, C.; Xu, Y.; García-Simón, C.; Gómez, L.; Juanhuix, J.; Gándara, F.; Imaz, I.; MasPOCH, D.; von Delius, M.; Ribas, X. *Nat. Chem.* **2021**, *13*, 420.
- Wachter, M.; Jurkiewicz, L.; Hirsch, A. *Chem. Eur. J.* **2021**, *27*, 7677.
- Pujals, M.; Pèlachs, T.; Fuertes-Espinosa, C.; Parella, T.; Garcia-Borràs, M.; Ribas, X. *Cell Rep. Phys. Sci.* **2022**, *3*, 100992.
- Kishi, N.; Akita, M.; Kamiya, M.; Hayashi, S.; Hsu, H. F.; Yoshizawa, M. *J. Am. Chem. Soc.* **2013**, *135*, 12976.
- Yamashina, M.; Yuki, T.; Sei, Y.; Akita, M.; Yoshizawa, M. *Chem. Eur. J.* **2015**, *21*, 4200.
- García-Simón, C.; Monferrer, A.; Garcia-Borràs, M.; Imaz, I.; MasPOCH, D.; Costas, M.; Ribas, X. *Chem. Commun.* **2019**, *55*, 798.
- Chen, B.; Holstein, J. J.; Horiuchi, S.; Hiller, W. G.; Clever, G. H. *J. Am. Chem. Soc.* **2019**, *141*, 8907.
- Chen, B.; Horiuchi, S.; Holstein, J. J.; Jacopo, T.; Clever, G. H. *Chem. Eur. J.* **2019**, *25*, 14921.
- Chen, B.; Holstein, J. J.; Platzek, A.; Schneider, L.; Wu, K.; Clever, G. H. *Chem. Sci.* **2022**, *13*, 1829.
- Hasegawa, S.; Meichsner, S. L.; Holstein, J. J.; Baksi, A.; Kananmascheff, M.; Clever, G. H. *J. Am. Chem. Soc.* **2021**, *143*, 9718.
- Yang, Y.; Ronson, T. K.; Lu, Z.; Zheng, J.; Vanthuyne, N.; Martinez, A.; Nitschke, J. R. *Nat. Commun.* **2021**, *12*, 4079.
- To the NMR tube where an acetonitrile solution of Pd₂1₄ (0.70 mM, 0.600 mL, 0.42 μmol) was placed, excess solid corannulene was added and heated at 70 °C for 24 h. ¹H NMR (500 MHz, CD₃CN, 298 K): δ (ppm) **e** 8.35 (s, 16 H), **d** 8.03 (d, J = 8.8 Hz, 8H), **f** 7.86 (m, 8 H), **b** 7.82 (m, 8 H), **c** 7.48 (dd, J = 8.8, 5.7 Hz, 8 H), **g** 7.36 (dd, J = 5.3, 3.3 Hz, 8 H), **h** 6.61 (s, 8 H), **a** 6.00 (s, 8H), **encapsulated corannulenes** 5.47 (s, 20 H). ¹³C NMR (125 MHz, CD₃CN, 298 K): δ (ppm) 166.12, 165.70, 154.15, 152.99, 151.33, 150.30, 148.64, 147.74, 142.88, 142.40, 139.94, 138.09, 133.29, 132.40, 131.49, 130.95, 130.35, 130.16, 128.66, 127.49, 126.89, 126.27, 125.91, 121.68, 120.64, 54.94, 54.54 (12 signals out of 13 signals from empty Pd₂1₄). **DOSY**: Diffusion coefficient *D* of corannulenes inside Pd₂1₄ and free corannulene in the same solution were estimated to be 6.69 × 10⁻¹⁰ and 18.58 × 10⁻¹⁰ m²·s⁻¹, respectively. **ESI MS** (positive): found: 724.6237; calculated for [(C₃₄H₁₈N₄O₄)₄Pd₂(C₂₀H₁₀)₂]⁴⁺ to be 724.6248
- Schmidt, B. M.; Osuga, T.; Sawada, T.; Hoshino, M.; Fujita, M. *Angew. Chem. Int. Ed.* **2015**, *55*, 1561.
- General procedure**: To an acetonitrile solution of Pd₂1₄ (0.35 mM, 1.0 mL, 0.35 μmol) in a vial was added an excess amount of solid guest. The heterogeneous mixture was stirred under heating at 70 °C for 24 h. After the reaction, the residual solid guest was removed by filtration. The yields were estimated from the ¹H NMR integral ratio.
2@Pd₂1₄: ¹H NMR (500 MHz, CD₃CN, 298 K): δ (ppm) **b** 8.38 (d, J = 5.2 Hz, 4 H), **b** 8.37 (d, J = 5.2 Hz, 4 H), **d** 8.32 (ddd, J = 8.5, 2.2, 1.2 Hz, 4 H), **d** 8.27 (ddd, J = 8.5, 2.2, 1.2 Hz, 4 H), **e*** 8.22 (s, 8 H), **e** 7.97 (s, 4 H), **e** 7.87 (s, 4 H), **c** 7.78 (dd, J = 8.5, 5.6 Hz, 4 H), **c** 7.74 (dd, J = 8.5, 5.6 Hz, 4 H), **f*** 7.73–7.64 (m, 8 H), **a** 7.34 (d, J = 2.1 Hz, 4 H), **g*** 7.26–7.20 (m, 8 H), **a** 7.10 (d, J = 2.1 Hz, 4 H), **h** 6.43 (s, 2 H), **h** 6.37 (s, 2 H), **h** 6.27 (s, 2 H), **h** 6.20 (s, 2 H), **i** 4.06 (s, 4 H), **j** 3.57 (s, 3 H). ¹³C NMR (150 MHz, CD₃CN, 298 K): δ (ppm) 166.15, 166.00, 165.71, 165.60, 154.38, 153.71, 153.49, 153.44, 153.30, 152.23, 152.15, 147.56, 147.45, 146.51, 146.10, 145.73, 145.18, 144.80, 144.15, 144.02, 143.35, 143.01, 142.99, 142.83, 142.81, 142.27, 142.13, 142.03, 141.02, 140.74, 140.28, 140.16, 138.79, 135.51, 132.62, 132.13, 131.09, 131.06, 130.96, 130.61, 129.45, 129.04, 127.76, 127.74, 127.70, 127.69, 126.24, 126.20, 126.16, 126.01, 121.91, 121.76, 121.58, 121.55, 71.41, 69.57, 54.77, 54.70, 54.58, 42.11. **DOSY**: Diffusion coefficient *D* = 5.26 × 10⁻¹⁰ m²·s⁻¹, and hydrodynamic radius *r*_H was calculated to be 12.4 Å. **ESI MS** (positive): found: 794.0999 and 1087.7986; calculated for [(C₃₄H₁₈N₄O₄)₄Pd₂(C₆₃NH₇)]⁴⁺ and [(C₃₄H₁₈N₄O₄)₄Pd₂(C₆₃NH₇)(BF₄)]³⁺ to be 794.1005 and 1087.8021, respectively.
3@Pd₂1₄: ¹H NMR (500 MHz, CD₃CN, 298 K): δ (ppm) **b** 8.63 (d, J = 5.2 Hz, 4 H), **b** 8.36 (d, J = 5.2 Hz, 4 H), **e** 8.32 (s, 4 H), **d** 8.28 (ddd, J = 8.5, 2.2, 1.2 Hz, 4 H), **d** 8.26 (ddd, J = 8.5, 2.2, 1.2 Hz, 4 H), **e** 8.12 (s, 4 H), **e** 8.07 (s, 4 H), **k**/l 7.99 (m, 2 H), **k**/l 7.94 (m, 2 H), **c** 7.80 (dd, J = 8.5, 5.6 Hz, 4 H), **e** 7.79 (s, 4 H), **c** 7.70 (dd, J = 8.5, 5.6 Hz, 4 H), **f*** 7.70–7.61 (m, 8 H), **a** 7.54 (d, J = 2.1 Hz, 4 H), **a** 7.50 (d, J = 2.1 Hz, 4 H), **g*** 7.26–7.17 (m, 8 H), **h** 6.50 (s, 2 H), **h** 6.37 (s, 2 H), **h** 6.20 (s, 2 H), **h** 6.15 (s, 2 H), **i** 4.44 (s, 2 H), **j** 3.04 (m, 1 H), **j** 2.71 (m, 1 H). ¹³C NMR (150 MHz, CD₃CN, 298 K): δ (ppm) 166.16, 166.13, 165.96, 165.68, 165.51, 156.20, 155.44, 153.78, 153.51, 153.36, 153.09, 153.01, 152.48, 151.80, 150.25, 148.66, 148.26, 147.15, 146.57, 146.51, 146.10, 145.71, 145.64, 145.52, 145.26, 145.01, 144.96, 144.76, 144.71, 144.19, 143.85, 143.84, 143.16, 143.11, 143.04, 143.02, 142.97, 142.85, 142.83, 142.61, 142.40, 142.34, 142.13, 142.03, 141.97, 141.13, 140.99, 140.72, 140.48, 140.47, 139.29, 138.21, 138.04, 137.23, 136.41, 132.94, 132.63, 132.48, 131.07, 131.03, 130.90, 130.68, 130.37, 129.42, 129.26, 129.23, 128.37, 127.70, 127.66, 127.53, 126.24, 126.22, 126.02, 125.96, 125.19, 121.83, 121.63, 121.59, 121.30, 120.71, 76.22, 58.71, 54.85, 54.79, 54.64, 54.48 (13 signals from empty Pd₂1₄). **DOSY**: Diffusion coefficient *D* = 5.47 × 10⁻¹⁰ m²·s⁻¹, and hydrodynamic radius *r*_H was calculated to be 12.0 Å. **ESI MS** (positive): found: 808.8505 and 1107.4664; calculated for [(C₃₄H₁₈N₄O₄)₄Pd₂(C₆₉H₈)]⁴⁺ and [(C₃₄H₁₈N₄O₄)₄Pd₂(C₆₉H₈)(BF₄)]³⁺ to be 808.8518 and 1107.4704, respectively.

4@Pd₂1₄: ¹H NMR (500 MHz, CD₃CN, 298 K): δ (ppm) **b** 8.60 (d, *J* = 5.2 Hz, 4 H), **b** 8.38 (d, *J* = 5.2 Hz, 4 H), **d** 8.33 (ddd, *J* = 8.5, 2.2, 1.2 Hz, 4 H), **d** 8.31 (ddd, *J* = 8.5, 2.2, 1.2 Hz, 4 H), **e** 8.24 (s, 4 H), **n** 8.12 (m, 2 H), **e*2** 8.09 (s, 8 H), **e** 7.90 (s, 4 H), **o** 7.89 (m, 1 H) **c** 7.81 (dd, *J* = 8.5, 5.6 Hz, 4 H), **c** 7.76 (dd, *J* = 8.5, 5.6 Hz, 4 H), **f*4&m** 7.74–7.61(m, 10 H), **a** 7.56 (d, *J* = 2.1 Hz, 4 H), **a** 7.54 (d, *J* = 2.1 Hz, 4 H), **g*4** 7.26–7.18 (m, 8 H), **h** 6.45(s, 2 H), **h** 6.33 (s, 2 H), **h** 6.32 (s, 2 H), **h** 6.19 (s, 2 H), **i** 3.68 (s, 3 H), **j** 2.52 (m, 2 H), **l** 2.31 (m, 2 H), **k** 2.00 (m, 2 H). ¹³C NMR (176 MHz, CD₃CN, 298 K): δ (ppm) 174.35, 166.17, 166.01, 165.96, 165.68, 165.57, 153.66, 153.65, 153.52, 153.45, 153.11, 152.61, 151.93, 150.26, 149.26, 148.70, 148.12, 147.44, 145.07, 144.91, 144.79, 144.33, 144.12, 144.09, 144.07, 143.96, 143.86, 143.48, 143.24, 143.18, 143.09, 142.99, 142.93, 142.82, 142.80, 142.72, 142.68, 142.62, 142.52, 142.21, 142.05, 141.86, 141.71, 141.59, 140.86, 140.72, 140.70, 140.54, 140.47, 140.41, 139.70, 138.05, 136.80, 136.62, 135.72, 132.88, 132.71, 132.63, 132.51, 131.11, 131.07, 131.03, 130.73, 130.39, 130.33, 130.11, 129.61, 129.24, 128.39, 127.76, 127.73, 127.55, 126.35, 126.25, 126.20, 125.98, 121.73, 121.59, 120.77, 120.72, 81.63, 54.81, 54.72, 54.66, 54.52, 54.50, 54.35, 52.21, 34.41, 33.80, 23.42 (13 signals from empty Pd₂1₄). **DOSY**: Diffusion coefficient *D* = 5.38 × 10⁻¹⁰ m²·s⁻¹, and hydrodynamic radius *r_H* was calculated to be 12.1 Å. **ESI MS** (positive): found: 827.3594 and 1132.1460; calculated for [(C₃₄H₁₈N₄O₄)₄Pd₂(C₇₂H₁₄O₂)]⁴⁺ and [(C₃₄H₁₈N₄O₄)₄Pd₂(C₇₂H₁₄O₂)(BF₄)]³⁺ to be 827.3610 and 1132.1494, respectively.

(28) Yoshizawa, M.; Klosterman, J. K.; Fujita, M. *Angew. Chem. Int. Ed.* **2009**, *48*, 3418.